# Discovery and Functional Analysis of a Salicylic Acid Hydroxylase from *Aspergillus niger*

Ronnie J. M. Lubbers,[a] Adiphol Dilokpimol,[a] Jaap Visser,[a] Kristiina S. Hildén,[b] Miia R. Mäkelä,[b] Ronald P. de Vries[a]

[a]Fungal Physiology, Westerdijk Fungal Biodiversity Institute & Fungal Molecular Physiology, Utrecht University, Utrecht, The Netherlands
[b]Department of Microbiology, University of Helsinki, Helsinki, Finland

**ABSTRACT** Salicylic acid plays an important role in the plant immune response, and its degradation is therefore important for plant-pathogenic fungi. However, many nonpathogenic microorganisms can also degrade salicylic acid. In the filamentous fungus *Aspergillus niger*, two salicylic acid metabolic pathways have been suggested. The first pathway converts salicylic acid to catechol by a salicylate hydroxylase (ShyA). In the second pathway, salicylic acid is 3-hydroxylated to 2,3-dihydroxybenzoic acid, followed by decarboxylation to catechol by 2,3-dihydroxybenzoate decarboxylase (DhbA). *A. niger* cleaves the aromatic ring of catechol catalyzed by catechol 1,2-dioxygenase (CrcA) to form *cis,cis*-muconic acid. However, the identification and role of the genes and characterization of the enzymes involved in these pathways are lacking. In this study, we used transcriptome data of *A. niger* grown on salicylic acid to identify genes (*shyA* and *crcA*) involved in salicylic acid metabolism. Heterologous production in *Escherichia coli* followed by biochemical characterization confirmed the function of ShyA and CrcA. The combination of ShyA and CrcA demonstrated that *cis,cis*-muconic acid can be produced from salicylic acid. In addition, the *in vivo* roles of *shyA*, *dhbA*, and *crcA* were studied by creating *A. niger* deletion mutants which revealed the role of these genes in the fungal metabolism of salicylic acid.

**IMPORTANCE** Nonrenewable petroleum sources are being depleted, and therefore, alternative sources are needed. Plant biomass is one of the most abundant renewable sources on Earth and is efficiently degraded by fungi. In order to utilize plant biomass efficiently, knowledge about the fungal metabolic pathways and the genes and enzymes involved is essential to create efficient strategies for producing valuable compounds such as *cis,cis*-muconic acid. *cis,cis*-Muconic acid is an important platform chemical that is used to synthesize nylon, polyethylene terephthalate (PET), polyurethane, resins, and lubricants. Currently, *cis,cis*-muconic acid is mainly produced through chemical synthesis from petroleum-based chemicals. Here, we show that two enzymes from fungi can be used to produce *cis,cis*-muconic acid from salicylic acid and contributes in creating alternative methods for the production of platform chemicals.

**KEYWORDS** catechol-dioxygenase, chemical building block, intradiol ring fission, platform chemical, salicylic acid metabolism

Salicylic acid (2-hydroxybenzoic acid) plays an important role in the regulation of the plant defense response against pathogens (1, 2). Many pathogenic fungi are able to degrade salicylic acid to manipulate the plant defense response. However, nonpathogenic fungi also have the ability to degrade salicylic acid. In several *Aspergillus* species, two salicylic acid metabolic pathways resulting in the formation of catechol have been reported (3–6). In the first pathway, salicylic acid is decarboxylated to catechol by salicylate hydroxylase (decarboxylating) (ShyA). In the second pathway, salicylic

Address correspondence to Ronald P. de Vries, r.devries@wi.knaw.nl.

acid is 3-hydroxylated to 2,3-dihydroxybenzoic acid, which is converted to catechol through decarboxylation by 2,3-dihydroxybenzoic acid decarboxylase (DhbA) (7). The aromatic ring of catechol is cleaved by a catechol 1,2-dioxygenase (CrcA), resulting in the formation of *cis,cis*-muconic acid. *cis,cis*-Muconic acid is further converted through the oxoadipate pathway to acetyl coenzyme A (acetyl-CoA) and succinate, which enter the tricarboxylic acid cycle. Current interest in this pathway consists of the fact that *cis,cis*-muconic acid can be used as a platform chemical that can serve as a precursor to adipic acid and terephthalic acid. These compounds are used for the synthesis of nylon and other valuable materials, such as polyethylene terephthalate (PET), polyurethane, resins, and lubricants (8–10). Currently, *cis,cis*-muconic acid is mainly produced through chemical synthesis from petroleum-based chemicals (11). However, several methods have been developed to produce biobased *cis,cis*-muconic acid using microorganisms (8, 12–15).

In the ascomycete fungi *Fusarium graminearum* and *Epichloë festucae*, salicylate hydroxylases (decarboxylating) have been identified (16–18), while in *Aspergillus nidulans*, four genes were suggested to encode salicylate hydroxylase (decarboxylating), DhbA, salicylate 3-hydroxylase, and CrcA, respectively, but their function has not been confirmed (5). In *A. niger*, DhbA has been enzymatically characterized, but its role in aromatic metabolism has not been studied (7). In addition, four intradiol dioxygenases have been characterized from *A. niger*, three of which are able to cleave catechol to *cis,cis*-muconic acid (19, 20). One of these intradiol dioxygenases was identified as hydroxyquinol 1,2-dioxygenase (HqdA) (20). Currently, the *in vivo* role of catechol 1,2-dioxygenase remains to be proven.

In this study, we identified the genes encoding ShyA, DhbA, and CrcA of *A. niger* and demonstrated that recombinant ShyA and CrcA together can efficiently convert salicylic acid into *cis,cis*-muconic acid through catechol as an intermediate. Deletion of *shyA*, *dhbA*, and *crcA* in *A. niger* resulted in reduced growth on salicylic acid, 2,3-dihydroxybenzoic acid, and catechol, respectively, confirming their *in vivo* roles.

## RESULTS

**Identification of the salicylic acid hydroxylase, 2,3-dihydroxybenzoic acid decarboxylase, and catechol 1,2-dioxygenase from *A. niger*.** To identify genes involved in the metabolism of salicylic acid, transcriptome data of *A. niger* grown on salicylic acid for 2 h was used as reported previously (21). In the *A. niger* NRRL3 genome, 32 genes are annotated as putative salicylate 1-monooxygenase, but only two genes, NRRL3_9723 and NRRL3_43, were highly induced (fold change ≥ 4) by salicylic acid compared to the control (see Table S1 in the supplemental material). NRRL3_9723 showed high amino acid similarity to Shy1 from *F. graminearum* (FgShy1) (16) (65.1%) and to a putative salicylate hydroxylase (AN2114) from *A. nidulans* (5) (77.3%), while NRRL3_43 is less similar to these two enzymes (38.8% and 31.6%, respectively). In addition, NRRL3_9723 has a 37.2% sequence similarity to *Pseudomonas putida* NahG, while NRRL3_43 is 25.3% similar. Therefore, NRRL3_9723 was selected as the putative ShyA of *A. niger*.

BLASTP analysis of a suggested salicylate 3-hydroxylase from *A. nidulans* (5) (AN7418) revealed 21 homologs in *A. niger*. While NRRL3_43 did not have the highest amino acid similarity to AN7418, it was the only gene that was induced by salicylic acid (Table 1 and Table S2). All three intradiol ring cleavage dioxygenases (HqdA, NRRL3_4787, and NRRL3_5330) were induced by salicylic acid compared to the control. The highest induction was observed for NRRL3_4787, which was therefore selected for further investigation as the putative CrcA of *A. niger* (Table 1).

**Colorimetric assay revealed salicylate hydroxylase activity of ShyA on salicylic acid.** To confirm the salicylate hydroxylase activity of the candidate ShyA, *Escherichia coli* strains that produce recombinant ShyA were inoculated on plates containing 1 mM salicylic acid together with an *E. coli* strain containing the empty vector (negative control). After 2 days, plates containing the recombinant strains (ShyA.1 and ShyA.2) turned brown, while the medium of the empty vector control strain remained yellow (Fig. 1a).

**TABLE 1** Expression of candidate salicylic acid metabolic genes on salicylic acid compared to a no-carbon-source control[a]

| JGI database gene ID | Annotation according to JGI database | Described protein | FPKM SA | NC | Deseq2 fold change | P value[b] |
|---|---|---|---|---|---|---|
| NRRL3_9723 | FAD-dependent oxidoreductase | | 225.70 | 11.14 | 20.03 | 0.000 |
| NRRL3_43 | FAD-binding domain-containing protein | | 1350.53 | 134.09 | 9.84 | 0.000 |
| NRRL3_4385 | Amidohydrolase | 2,3-Dihydroxybenzoate decarboxylase (DhbA) | 2903.69 | 1406.88 | 2.03 | 0.041 |
| NRRL3_2597 | FAD-binding domain-containing protein | | 0.69 | 0.25 | 2.64 | 0.103 |
| NRRL3_4787 | Intradiol ring cleavage dioxygenase | | 2804.74 | 343.56 | 8.00 | 0.001 |
| NRRL3_5330 | Intradiol ring cleavage dioxygenase | | 46.85 | 15.05 | 2.98 | 0.000 |
| NRRL3_2644 | Intradiol ring cleavage dioxygenase | Hydroquinol 1,2-dioxygenase (HqdA) | 77.16 | 25.25 | 3.01 | 0.000 |
| NRRL3_8551 | FAD-binding domain-containing protein | *p*-Hydroxybenzoate-*m*-hydroxylase (PhhA) | 16.96 | 69.70 | 0.24 | 0.000 |
| NRRL3_1405 | Intradiol ring cleavage dioxygenase | Protocatechuic acid 3,4-dioxygenase (PrcA) | 8.61 | 59.02 | 0.15 | 0.001 |

[a]Abbreviations: ID, identifier; FPKM, fragments per kilobase per million; SA, salicylic acid; NC, no-carbon-source control.
[b]P values were calculated using Deseq2 software (51).

Degradation of salicylic acid was further determined by a colorimetric assay. This degradation resulted in the purple coloration of salicylic acid in the negative-control plate, while the plates with the recombinant ShyA *E. coli* strains turned black (Fig. 1a).

A similar experiment was performed in liquid cultures, resulting in the brown color formation in the two strains expressing *shyA* (Fig. 1b), indicating conversion of salicylic acid to catechol (Fig. 1c). These results confirm that NRRL3_9723 encodes the salicylate hydroxylase ShyA.

**Production of *cis,cis*-muconic acid using recombinant ShyA and CrcA.** To confirm the role of ShyA and CrcA in *cis,cis*-muconic acid production, both were produced in *E. coli*. The *E. coli* strain expressing *hqdA* was obtained from Lubbers et al. (20). DhbA was not included since it has been previously characterized (7). Cell-free extracts of *E. coli* ShyA.1, CrcA, HqdA, and the empty vector control strain were incubated with 0.25 mM salicylic acid at 30°C overnight, after which the reaction mixtures were analyzed by high-performance liquid chromatography (HPLC).
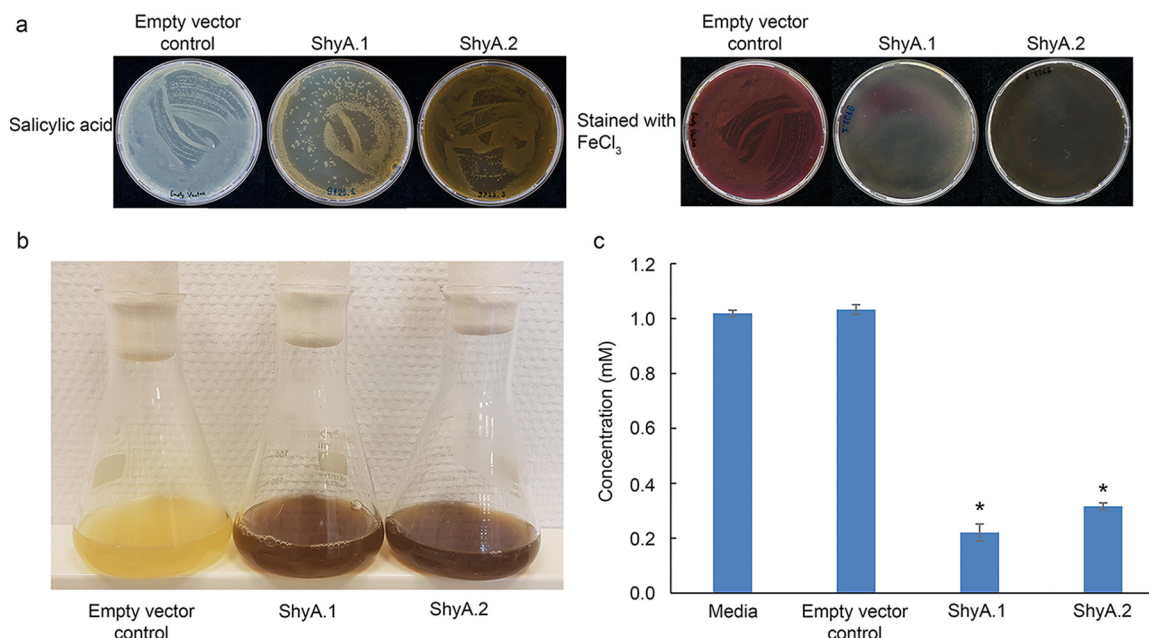


**FIG 1** Expression of *A. niger shyA* in two independent *E. coli* strains, ShyA.1 and ShyA.2. (a and b) LB plates (a) and liquid cultures (b) contained 1 mM salicylic acid and were incubated for 2 days. An *E. coli* strain containing the empty vector without an insert was used as a control. After incubation, the plates were stained with FeCl₃, coloring salicylic acid purple and catechol black. (c) Salicylic acid concentrations in culture medium were determined by HPLC. Error bars represent the standard deviations of three biological replicates. Asterisks indicate significant differences in salicylic acid concentration compared with the empty vector control (Student's *t* test, *P* value ≤ 0.01).
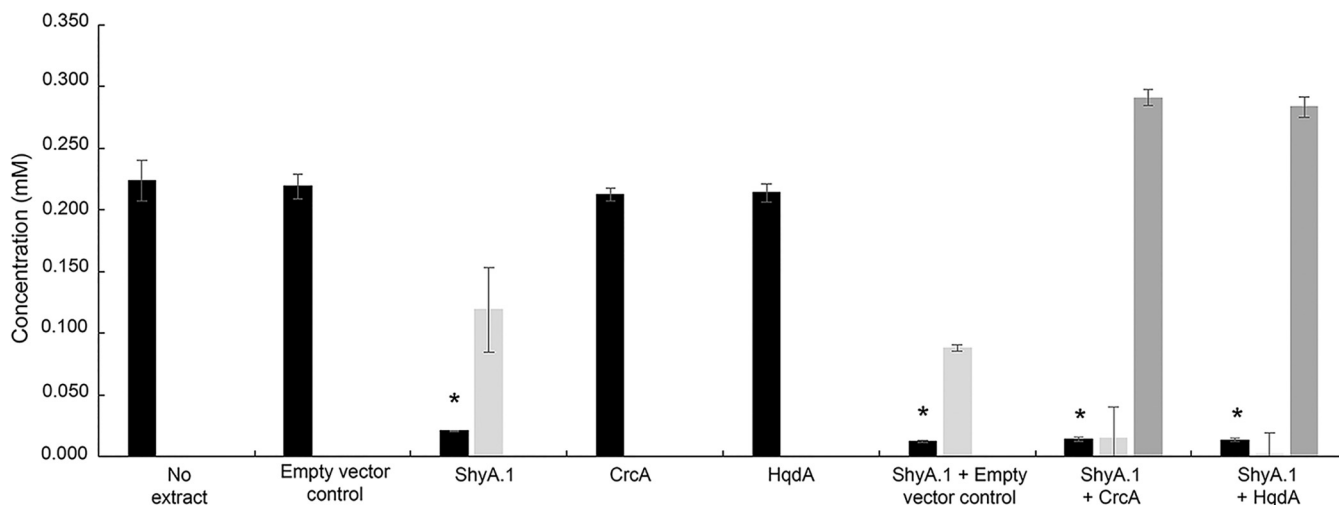
**FIG 2** Conversion of salicylic acid by cell extracts of the *E. coli* strains producing ShyA, CrcA, and HqdA from *A. niger*. Black, light gray, and dark gray bars represent salicylic acid, catechol, and *cis,cis*-muconic acid, respectively. The concentration of *cis,cis*-muconic acid was slightly overestimated due to the impurity of the standard. Error bars represent the standard deviations of three biological replicates. Asterisks indicate significant differences in salicylic acid concentration compared with the empty-vector control (Student's *t* test, *P* value ≤ 0.01).

Salicylic acid (0.25 mM) was converted to catechol (0.12 ± 0.04 mM) by the cell extracts from the *shyA* expression strain, whereas for the empty vector control and cell extracts of *crcA* and *hqdA* expression strains, no catechol was detected (Fig. 2). The cell extracts from the *crcA* or *hqdA* expression strain were verified to convert catechol to *cis,cis*-muconic acid (Fig. S1).

Incubation of salicylic acid by a combination of cell extracts from the *shyA* with the *crcA* or the *hqdA* overexpression strains resulted in the formation of *cis,cis*-muconic acid (Fig. 2), demonstrating that the combination of these enzymes is sufficient for this biochemical conversion. Almost no salicylic acid or catechol was detected, indicating that the conversion was highly efficient.

**Biochemical characterization of purified ShyA.** To investigate the biochemical properties of ShyA, the enzyme produced in *E. coli* was purified using immobilized-metal affinity chromatography. The calculated molecular mass of ShyA-HIS was 49.2 kDa and corresponded with the band observed by SDS-PAGE (Fig. S2). The optimal pH and temperature for activity were determined to be pH 5.6 to 6.0 (Fig. 3a) and 45 to 50°C (Fig. 3b), respectively. The kinetic profile of ShyA, obtained while only varying the salicylic acid concentration at a constant 1 mM concentration of the second substrate (NADH), did not follow Michaelis-Menten kinetics. It revealed an apparent $V_{max}$ of 75.6 ± 5.3 $\mu$mol/min/mg protein and a $K_{0.5}$ of approximately 138.8 ± 12.8 $\mu$M (Fig. 3c).

Salicylate hydroxylases are known to perform NADH oxidation reactions in the presence of pseudosubstrates, like benzoate, without hydroxylating such a compound (22, 23). In order to distinguish between the oxidase and hydroxylase activities, the reaction mixtures were analyzed by HPLC (Table 2). ShyA was active toward salicylic acid, 4-aminosalicylic acid, 2,3-dihydroxybenzoic acid, and gentisic acid, resulting into the formation of catechol, 4-aminocatechol, pyrogallol, and hydroxyquinol, respectively.

**ShyA, DhbA, and CrcA are involved in the fungal salicylic acid pathway.** To verify that the candidate genes encode the enzymes involved in the *in vivo* salicylic acid metabolic pathway of *A. niger*, six deletion mutants, the Δ*shyA*, Δ*dhbA*, Δ*crcA*, Δ43 (putative salicylate hydroxylase), Δ2597 (putative salicylate 3-hydroxylase), and Δ5330 (putative catechol 1,2-dioxygenase) mutants, were created. Cultivation on several aromatic compounds demonstrated that the growth of the Δ*shyA* mutant was reduced on salicylic acid but not on the other aromatic compounds tested (Fig. 4), confirming its role as the salicylate hydroxylase of *A. niger*. Growth of the Δ*dhbA* mutant was reduced on 2,3-dihydroxybenzoic acid but not on salicylic acid or catechol, confirming its
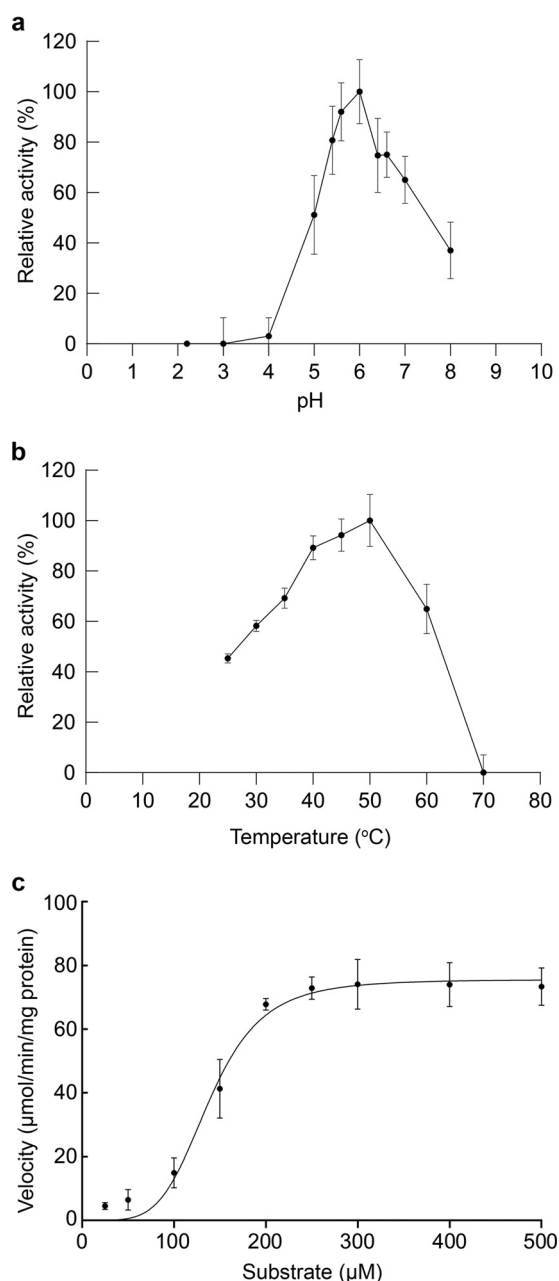
**FIG 3** Effects of pH and temperature on ShyA activity with 1 mM salicylic acid. (a). ShyA activity at 30°C after 15 min under different pH conditions; (b) ShyA activity at pH 6.0 after 15 min of incubation at different temperatures. Error bars represent the standard deviations between three replicates. (c) Rate of reaction of ShyA with salicylic acid. The assay was performed at pH 6.0 and 30°C. Error bars represent the standard deviations between three experiments.

metabolic role. Deletion of *crcA* resulted in growth similar to that of the no-carbon-source control on salicylic acid, 2,3-dihydroxybenzoic acid, and catechol, while deletion of NRRL3_5330 or *hqdA* did not result in a phenotype, indicating that *crcA* encodes the catechol 1,2-dioxygenase of *A. niger*. Growth of the Δ43, Δ5330, and Δ2597 mutants did not result in any phenotypes on the tested aromatic compounds.

When the plates containing salicylic acid, 2,3-dihydroxybenzoic acid, and catechol were stained with FeCl$_3$ (Fig. 5), the plates containing salicylic acid turned purple and halos were observed for the reference, Δ*dhbA*, Δ*hqdA*, Δ43, Δ5330, and Δ2597 strains. No halos were detected for the Δ*shyA* and Δ*crcA* mutants, indicating that salicylic acid is not converted in these strains. Plates containing 2,3-dihydroxybenzoic acid turned

**TABLE 2** Conversion of benzoic acids by ShyA[a]
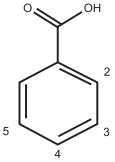


| Substrate | 2 | 3 | 4 | 5 | Substrate converted (%) |
|---|---|---|---|---|---|
| Salicylic acid | OH | H | H | H | >99 |
| 4-Aminosalicylic acid | OH | H | NH$_2$ | H | 72 |
| m-Hydroxybenzoic acid | H | OH | H | H | 0[a] |
| p-Hydroxybenzoic acid | H | H | OH | H | 0[a] |
| 2,3-Dihydroxbenzoic acid | OH | OH | H | H | 82 |
| Gentisic acid | OH | H | H | OH | 93 |
| Protocatechuic acid | H | OH | OH | H | 0[a] |
| Vanillic acid | H | OCH$_3$ | OH | H | 0[a] |
| Syringic acid | H | OCH$_3$ | OH | OCH$_3$ | 0[a] |
| Benzoic acid | H | H | H | H | 0[a] |

[a] No conversion after 16 h incubation.

[a]The reaction conditions using purified enzyme were as follows: 1 mM substrate, McIlvaine buffer (pH 6.0), 1 mM NADH, incubated at 30°C for 1 h. Conversion values were determined by HPLC. The structural differences of the substrates are indicated by the residues attached to the aromatic ring. A value of 0 indicates that there was no conversion after 16 h of incubation.

black after staining, and no halos were observed when *dhbA* and *crcA* were deleted. Catechol plates turned black and no halo was produced when *crcA* was deleted. These results confirmed the phenotypes of the growth profile (Fig. 4).

**Candidates of the oxoadipate pathway genes are highly induced by salicylic acid.** Further analysis of the *A. niger* transcriptome data revealed five additional genes that are highly induced (fold change ≥ 4) by salicylic acid (Table 3). Four of these genes are homologs of the oxoadipate pathway genes from *A. nidulans* (5). The final step of this pathway is the conversion of 3-oxoadipate-succinyl-CoA to acetyl-CoA and succinate by 3-oxoacyl CoA thiolase. Only one gene annotated as a 3-oxoacyl CoA thiolase (NRRL3_1526) was induced by salicylic acid and is possibly involved in the conversion of 3-oxoadipate-SCoA. In both the *A. nidulans* and *A. niger* genomes, the putative 3-oxoadipate enol-lactone hydrolase is located next to the putative catechol 1,2-dioxygenase. Interestingly, homologs of the putative muconate isomerase (AN3895 in *A. nidulans*, NRRL3_10508 in *A. niger*) and putative muconolactone isomerase (AN4061 in *A. nidulans*, NRRL3_10507 in *A. niger*) are also clustered in the *A. niger* genome but not in the genome of *A. nidulans*.

**Phylogenetic diversity of ShyA in filamentous fungi.** To study the presence of ShyA in other fungi, a phylogenetic analysis was performed on selected ascomycete and basidiomycete genomes (Table S3). A BLASTP search using ShyA as a query did not retrieve NRRL3_43 of *A. niger* or the characterized FgShyC (16) and FgNahG (18) of *F. graminearum*, and these were therefore added manually to the phylogenetic analysis. *A. niger* ShyA and *F. graminearum* FgShy1 were both located in the same clade (Fig. S3), in which homologs of *Aspergillus fumigatus*, *Aspergillus japonicus*, *A. nidulans*, *A. oryzae*, *Mycosphaerella graminicola*, *Podospora anserina*, *Talaromyces stipitatus*, and *Zymoseptoria pseudotritici* were also found. FgNahG was clustered with NRRL3_43, while ShyI of the basidiomycete fungus *Ustilago maydis* (24) was clustered with two uncharacterized salicylate hydroxylase-like proteins from *A. niger* (NRRL3_2207) and *F. graminearum* (11948). In addition, a salicylate 1-monooxygenase (SalA, 8711) of *A. nidulans*, involved in terbinafine resistance (25), showed homology with ShyA but is located in a different clade (Fig. S3).
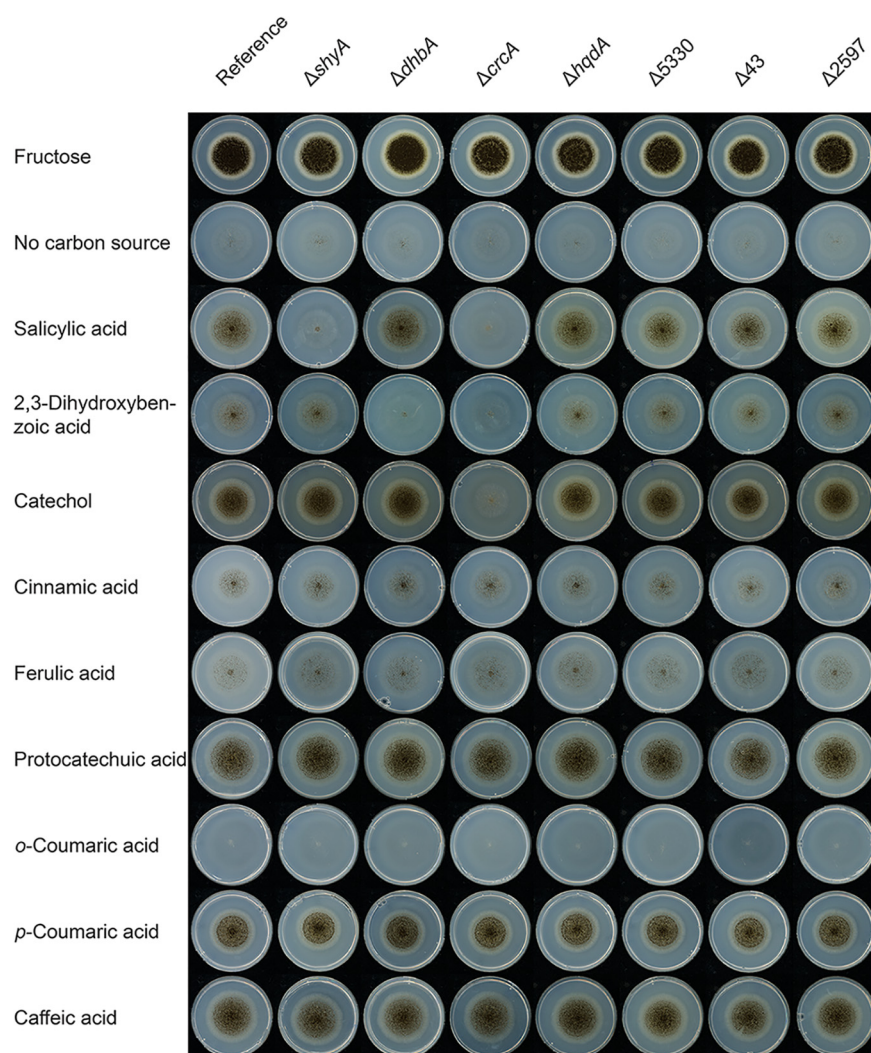
**FIG 4** Growth profile of the *A. niger* Δ*shyA*, Δ*dhbA*, Δ*crcA*, Δ*hqdA*, Δ43, Δ2597, and Δ5330 deletion mutants and the reference strain on aromatic compounds. Phenotypes were examined after 7 days at 30°C. Fructose and a no-carbon-source condition served as growth controls.

## DISCUSSION

The salicylic acid metabolic pathway in microorganisms has been studied for decades, but only a few fungal enzymes have been described (6), and the pathway is mainly studied for fungi in the context of plant pathogenicity (16, 24, 26, 27). In this study, we identified the genes encoding ShyA, DhbA, and CrcA using transcriptome data of *A. niger* grown on salicylic acid and showed that cell extracts containing ShyA and CrcA or purified ShyA and CrcA can be used to produce *cis,cis*-muconic acid from salicylic acid (Fig. 2 and Fig. S4). The optimal temperature (45 to 50°C) and optimal pH (5.6 to 6.0) of ShyA differ from those of the previously described salicylate hydroxylase NahG of *P. putida* (30°C and pH of 7.0 to 7.5) (23). In addition, we observed that ShyA shows activity on *o*-hydroxylated benzoic acids, such as 4-aminosalicylic acid, 2,3-dihydroxybenzoic acid, and gentisic acid, but not on benzoic acid derivatives that are not *o*-hydroxylated. Activities on *o*-hydroxylated substrates have also been observed for NahG (23). Surprisingly, characterization of ShyA revealed a sigmoidal curve. This may be caused by inhibition or inactivation due to low salicylate concentrations and relatively high NADH concentrations; the enzyme also exhibits NADH oxidase activity besides the more rapid hydroxylase activity (28).

The first step of the salicylic acid metabolic pathway of *A. niger* converting salicylic
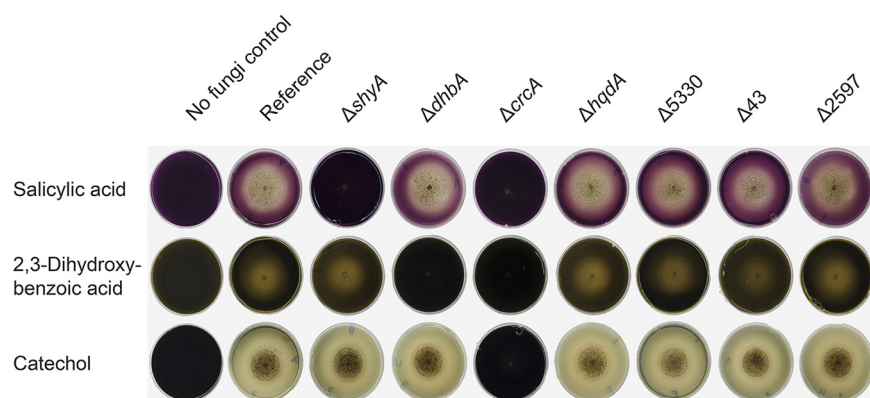
**FIG 5** Growth profile of the deletion strains and the reference on MM agar plates containing salicylic acid, 2,3-dihydroxybenzoic acid, and catechol after 7 days of growth and stained with $FeCl_3$. As a control, noninoculated plates were stained with $FeCl_3$.

acid to catechol is catalyzed by ShyA. The deletion of *shyA* results in severely reduced growth on salicylic acid, to a size similar to that of the no-carbon-source control. Based on the growth reduction, induction by salicylic acid, and the activity of the recombinant ShyA on salicylic acid, we conclude that NRRL3_9723 encodes the salicylate hydroxylase of *A. niger*. In contrast, in *F. graminearum*, FgShy1, which has activity on salicylic acid, and its corresponding gene, which is induced by salicylic acid, are considered not essential for growth on salicylic acid (16, 27, 29). Therefore, an additional salicylate hydroxylase was suggested. Despite the high induction of NRRL3_43 by salicylic acid, deletion of this gene did not result in a phenotype on salicylic acid. No other putative salicylate hydroxylases were induced by salicylic acid, indicating that no additional salicylate hydroxylases are present in *A. niger*. Therefore, we suggest that NRRL3_43 is a salicylic acid hydroxylase-like enzyme. Interestingly, FgNahG of *F. graminearum* also possesses salicylate hydroxylase activity and is, unlike FgShy1, essential for growth on salicylic acid (16, 18). However, the closest FgNahG homolog in *A. niger* is NRRL3_43 (58.3%), which is less similar to ShyA (40.5%) and FgShy1 (34.0%). In addition, FgNahG was not found as a homolog in the phylogenetic analysis. A recent review revealed that NRRL3_43 is part of a biosynthetic gene cluster in *A. niger*, but it is unknown which secondary metabolite is formed by this cluster (30). Further investigation of the transcriptome data showed that NRRL3_43 and 10 neighboring genes (NRRL3_35 to NRRL3_45) in the *A. niger* genome were induced by salicylic acid (Table S4). In the *Fusarium* genome, FgNahG appears not to be part of a secondary metabolic cluster, which indicates that no homolog of FgNahG is present in the *A. niger* genome.

The second salicylic acid metabolic pathway is the 3-hydroxylation of salicylic acid to 2,3-dihydroxybenzoic acid, which has been reported for *A. niger*, *A. nidulans*, and other fungi (26, 31), but the enzyme responsible for this conversion had not been

**TABLE 3** Expression of candidate oxoadipate pathway genes on salicylic acid compared to a no-carbon-source control

| JGI database gene ID | Annotation according to JGI database | Suggested function | Homolog of *A. nidulans*[a] | Amino acid similarity (%) | FPKM | | Deseq2 fold change | *P* value[b] |
|---|---|---|---|---|---|---|---|---|
| | | | | | SA | NC | | |
| NRRL3_10508 | Predicted L-carnitine dehydratase/ alpha-methylacyl-CoA racemase | Muconate isomerase | AN3895 | 80.0 | 1933.05 | 132.57 | 14.20 | 0.00 |
| NRRL3_10507 | Hypothetical protein | Muconolactone isomerase | AN4061 | 72.0 | 1888.93 | 158.93 | 11.58 | 0.00 |
| NRRL3_4788 | Predicted alpha/beta hydrolase | 3-Oxoadipate enol-lactone hydrolase | AN4531 | 70.1 | 1069.90 | 242.36 | 4.32 | 0.00 |
| NRRL3_1886 | 3-Oxoacid CoA-transferase | Succinyl-CoA:3-oxoadipate CoA-transferase | AN10495 | 86.5 | 131.90 | 8.00 | 16.13 | 0.00 |
| NRRL3_1526 | 3-Oxoacyl CoA thiolase | 3-Oxoacyl CoA thiolase | AN5698 | 91.2 | 306.30 | 47.39 | 6.38 | 0.00 |

[a]Protein IDs correspond to those in the AspGD database (http://aspgd.org/).
[b]The *P* values were calculated using Deseq2 software (51).
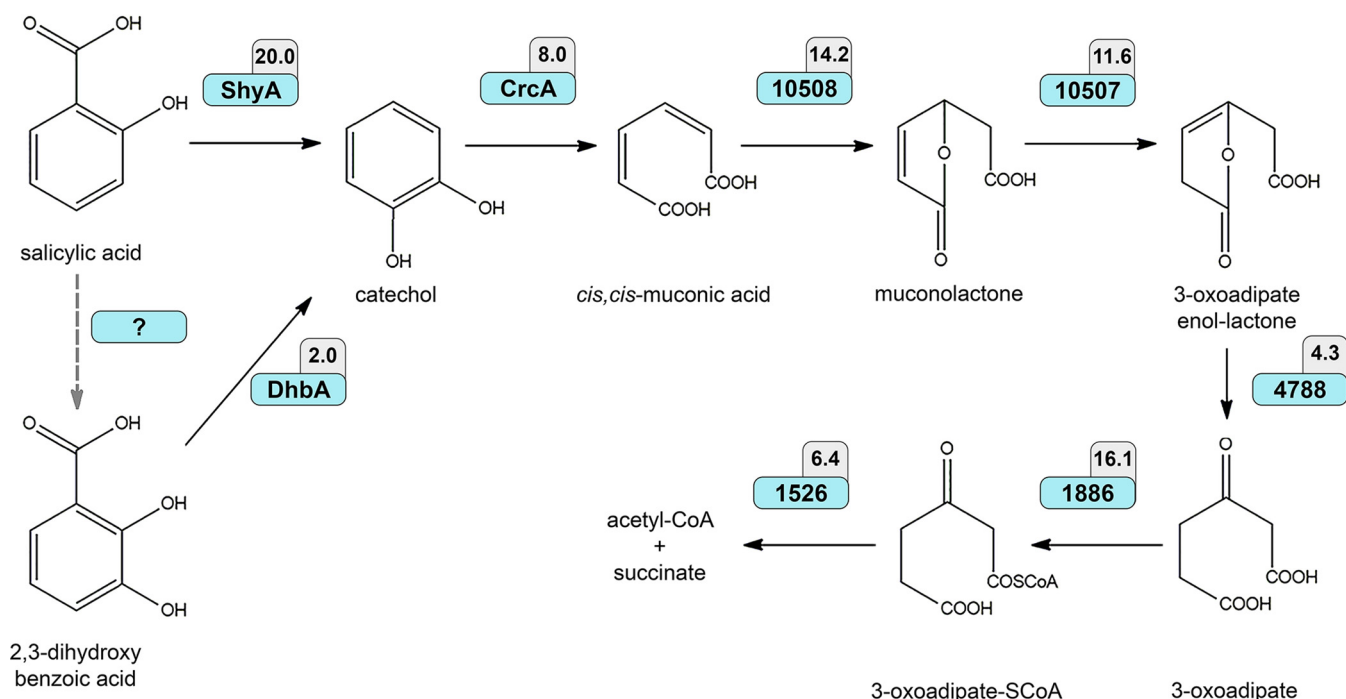
**FIG 6** The salicylic acid metabolic pathway and oxoadipate pathway in *A. niger*. Confirmed pathways are shown with black arrows, and the suggested *m*-hydroxylation pathway is shown with a gray dashed arrow. Boxed in gray are the gene expression fold change values on salicylic acid compared to the no-carbon-source control for the corresponding gene. NRRL3_10508, putative muconate isomerase; NRRL3_10507, putative muconolactone isomerase; NRRL3_4788, putative 3-oxoadipate enol-lactone hydrolase; NRRL3_1886, putative 3-oxoadipate CoA transferase; NRRL3_1526, putative 3-oxoacyl CoA thiolase.

demonstrated. In *Arabidopsis thaliana*, a salicylate 3-hydroxylase has been characterized (32). BLASTP analysis of this plant protein sequence against the *A. niger* NRRL3 genome resulted in 13 hits, none of which were induced by salicylic acid (Table S5). Therefore, this did not provide any leads for the identification of the gene encoding this enzyme. The second metabolic step in this pathway is the nonoxidative decarboxylation of 2,3-dihydroxybenzoic acid to catechol, which is catalyzed by DhbA. Deletion of *dhbA* in *A. niger* resulted in reduced growth on 2,3-dihydroxybenzoic acid, confirming the previously reported characterization (7). However, the deletion of *dhbA* did not result in reduced growth on salicylic acid, even though *dhbA* was induced by salicylic acid. This has also been observed in the fungal species *Trichosporon cutaneum* (33). In *F. graminearum*, deletion of the 2,3-dihydroxybenzoic acid decarboxylase resulted in delayed salicylic acid uptake, but no growth effect was detected on salicylic acid (27). If the *in vitro* activity of ShyA on 2,3-dihydroxybenzoic acid, resulting in the formation of pyrogallol, is also present *in vivo*, this would compete with the conversion of 2,3-dihydroxybenzoic acid to catechol mediated by DhbA. Therefore, we have strong indications that the 3-hydroxylation of salicylic acid plays either a minor or no role in the metabolism of salicylic acid in *A. niger* (Fig. 6).

Recently, three putative intradiol dioxygenases have been shown to convert catechol to *cis,cis*-muconic acid (19, 20), but HqdA was not involved in degradation of catechol *in vivo* (20). However, it remained unknown which of the remaining two enzymes corresponds to the true catechol 1,2-dioxygenase of *A. niger*, as both were induced on salicylic acid. Deletion of *crcA* resulted in severely reduced growth on catechol, similar to the no-carbon-source control, while deletion of NRRL3_5330 or *hqdA* did not result in any phenotype. In addition, the FeCl$_3$ assay of the catechol plates with the Δ*crcA* mutant did not produce a halo, which indicated that NRRL3_5330 or *hqdA* does not have an *in vivo* function as a catechol 1,2-dioxygenase-encoding gene in *A. niger*. Based on the deletion mutant, biochemical characterization, transcriptome data, and the previously characterized CrcA (19), we can conclude that NRRL3_4787 encodes this

enzyme in *A. niger*. The biological function of NRRL3_5330 remains unknown, but it has been shown to convert several catechol derivatives, including hydroxyquinol (19).

The ability to degrade salicylic acid has been suggested to be important for the pathogenicity of fungi on plants (16, 17, 24, 27). A connection between the pathogenicity and salicylic acid degradation by salicylate hydroxylase was demonstrated in *F. graminearum* by deleting FgNahG (18). In our phylogenetic study, we observed that many fungi, including non-plant-pathogenic species, are equipped with putative salicylic acid hydroxylases. Therefore, the ability to degrade salicylic acid appears to also be important for biological processes other than pathogenicity. Studies have shown that salicylic acid is released from plant residues and is found in soil (34–37). Salicylic acid has antifungal properties (38), which is a possible explanation for the presence of salicylic acid metabolism in non-plant-pathogenic fungi. Another possible explanation is that this pathway is part of the degradation of polycyclic aromatic hydrocarbons such as naphthalene, phenanthrene, and carbaryl (39, 40).

The identification and characterization of the *A. niger* enzymes ShyA and CrcA contribute to a better understanding of fungal aromatic metabolic pathways. We demonstrated that whole-genome transcriptome analysis is a powerful tool for studying metabolic pathways and identifying genes. The combination of recombinant ShyA and CrcA is an example of production of valuable compounds from this pathway, such as *cis*,*cis*-muconic acid, which is an important platform chemical for synthesis of plastic and resins. Understanding the metabolic pathway and the corresponding enzymes is essential for the creation of efficient fungal cell factories for conversion of renewable and sustainable resources, such as lignin, to valuable chemical building blocks.

## MATERIALS AND METHODS

**Candidate gene identification.** To identify candidate genes involved in salicylic acid metabolism, transcriptome data of *A. niger* N593 Δ*kusA* grown on 2 mM salicylic acid for 2 h and on minimal medium (MM) (41) without a carbon source (as a control) were obtained from Lubbers et al. (21). Genes were considered induced by using a cutoff of fragments per kilobase per million (FPKM) of $\geq 10$, fold change of $\geq 4$, and *P* value of $\leq 0.01$.

To identify the salicylate hydroxylase of *A. niger*, all genes annotated as salicylate 1-monooxygenase in the *A. niger* NRRL3 genome (https://mycocosm.jgi.doe.gov/Aspni_NRRL3_1) were obtained from the MycoCosm genome database. To reduce the number of candidates, BLASTP analysis was performed using the amino acid sequence of FgShy1 from *F. graminearum* (16), putative salicylate hydroxylase (AN2114 [http://www.aspergillusgenome.org/cgi-bin/locus.pl?locus=AN2114&organism=A_nidulans_FGSC_A4]) from *A. nidulans*, and the salicylate hydroxylase (NahG) (UniProt accession number P23262) of the bacterium *Pseudomonas putida*. To identify *dhbA*, the amino acid sequence of DhbA (7) was used as query in a BLASTP search against the *A. niger* NRRL3 genome. This resulted in the identification of a single gene (NRRL3_4385), which has been annotated as an amidohydrolase. For the identification of salicylate 3-hydroxylases, the amino acid sequence of a suggested salicylate 3-hydroxylase from *A. nidulans* (5) (AN7418 [http://www.aspergillusgenome.org/cgi-bin/locus.pl?locus=AN7418&organism=A_nidulans_FGSC_A4]) was used as a query in a BLASTP search against the *A. niger* NRRL3 genome.

**Construction of expression plasmids.** Full-length *shyA* was synthesized based on the reference sequence (NRRL3_9723) in pET23b containing a C-terminal hexa-His tag (Genscript Biotech, Leiden, the Netherlands). The expression plasmid for *crcA* containing an N-terminal hexa-His tag was created by inserting the gene in pET28a through homologous recombination as described previously (42). The plasmid was amplified from pET28a flanking the multiple-cloning site. The CrcA-encoding gene was amplified from cDNA of *A. niger* grown in salicylic acid. Purification of the PCR fragments and transformation of *E. coli* TOP10 were performed as described previously (20). The plasmid was isolated and verified for correctness by sequencing. Both plasmids were used to transform the *E. coli* protein production strain BL21(DE3) (New England BioLabs, Ipswich, MA).

**Protein production and purification.** Production and purification of the recombinant ShyA and CrcA proteins were performed as previously described (20). *E. coli* BL21(DE3) harboring pET23b-*shyA* or pET28a-*crcA* was grown in 10 ml of LB medium supplemented with 50 $\mu$g/ml of ampicillin for pET23b-*shyA* or 50 $\mu$g/ml of kanamycin for pET28a-*crcA* overnight at 37°C and 160 rpm. One milliliter of inoculum was transferred to a 1-liter Erlenmeyer flask containing 400 ml of LB medium supplemented with 50 $\mu$g/ml of ampicillin or kanamycin and grown to an optical density at 600 nm ($OD_{600}$) of 0.4 to 0.8. To induce recombinant protein production, isopropyl-$\beta$-D-thiogalactopyranoside (IPTG) with a final concentration of 100 $\mu$M was added to the cultures, which were further incubated overnight at 12°C and 160 rpm. Proteins were isolated and purified with a HisTrap FF 1-ml column coupled with the ÄKTA start system (GE Healthcare Life Sciences, Uppsala, Sweden) using the setup described previously (20). After purification, 0.5 mM flavin adenine dinucleotide (FAD) was added to the fractions containing ShyA.

The molecular mass of ShyA and CrcA was calculated *in silico* (https://www.bioinformatics.org/sms/

**TABLE 4** *A. niger* strains used in this study

| Strain | CBS no. | Genotype | Reference |
|---|---|---|---|
| N593 Δ*kusA* | CBS 138852 | *cspA1 pyrG* Δ*kusA*::*amdS* | 47 |
| Reference | CBS 145984 | *cspA1 pyrG* Δ*kusA*::*amdS* Δ*pyrG*::*pyrG* | This study |
| Δ*hqdA* | CBS 145839 | *cspA1 pyrG* Δ*kusA*::*amdS* Δ*hqdA*::*pyrG* | 20 |
| Δ*shyA* (9723) | CBS 146179 | *cspA1 pyrG* Δ*kusA*::*amdS* Δ*shyA*::*pyrG* | This study |
| Δ*dhbA* (4385) | CBS 146180 | *cspA1 pyrG* Δ*kusA*::*amdS* Δ*dhbA*::*pyrG* | This study |
| Δ*crcA* (4787) | CBS 146181 | *cspA1 pyrG* Δ*kusA*::*amdS* Δ*crcA*::*pyrG* | This study |
| Δ43 | CBS 146183 | *cspA1 pyrG* Δ*kusA*::*amdS* Δ43::*pyrG* | This study |
| Δ2597 | CBS 146182 | *cspA1 pyrG* Δ*kusA*::*amdS* Δ2597::*pyrG* | This study |
| Δ5330 | CBS 146184 | *cspA1 pyrG* Δ*kusA*::*amdS* Δ5330::*pyrG* | This study |

prot_mw.html) and estimated by SDS-PAGE (12% [wt/vol] polyacrylamide gel, Mini-PROTEAN Tetra Cell; Bio-Rad, Hercules, CA) using the Precision Plus prestained protein standards (Bio-Rad) as a marker. Protein concentrations were determined from the SDS-PAGE gel, using bovine serum albumin as standard, and quantified by ImageJ software (43).

**Enzyme activity assay of ShyA.** Activity assays were performed using cell extracts of *E. coli* BL21 expressing *shyA*, *crcA*, and *hqdA*, respectively. The *E. coli hqdA* expressing strain was obtained from Lubbers et al. (20). Cell-free extracts of *E. coli* BL21 harboring an empty vector were used as a negative control. The reaction mixture contained 100 $\mu$M phosphate buffer (pH 6.4), 200 $\mu$M substrate, and 40 $\mu$l of cell extract. Reaction mixtures were incubated for 1 h at 30°C, after which the reaction was stopped by incubation at 80°C for 10 min and analyzed with an HPLC (Dionex ICS-5000+ chromatography system; Thermo Scientific, Sunnyvale, CA) equipped with an Acclaim Mixed-Mode WAX-1 LC column (3 by 150 mm; Thermo Scientific) and a UV detector (225 nm; Thermo Scientific). The chromatographic separation was carried out using isocratic elution of 30°C at a flow rate of 0.425 ml/min with 25 mM potassium monophosphate and 0.8 mM pyrophosphate (pH 6.0) in 50% acetonitrile (44). Salicylic acid, catechol, and *cis,cis*-muconic acid standards were used as a reference.

Activity assay of purified ShyA with 1 mM concentrations of substrates were performed in 200-$\mu$l reaction mixtures that contained 1 mM NADH and McIlvaine buffer (pH 6.0) (45). After 3 h of incubation at 30°C, 100 $\mu$l of reaction mixture was diluted 10 times with acetonitrile and analyzed by HPLC.

A preliminary kinetic analysis of purified ShyA was carried out by varying the salicylic acid concentration between 25 and 500 $\mu$M at a fixed concentration of 1 mM NADH. A 96-well plate containing a fixed amount of McIlvaine buffer (pH 6.0) and various amounts of salicylic acid and demi water up to a total volume of 176 $\mu$l per well was preheated at 30°C. Then, 4 $\mu$l (total concentration of approximately 0.7 $\mu$g) of purified ShyA enzyme was added to the wells. The extract from the empty-vector-containing *E. coli* strain was used as a control. To start the reactions, 20 $\mu$l of 10 mM NADH was automatically injected with a FLUOstar Optima microplate reader (BMG Labtech, Ortenberg, Germany) with a preheated chamber at 30°C. Absorbance was measured every 2 s at 340 nm for 500 s. The $K_{0.5}$ (substrate concentration for half-saturation) and $V_{max}$ were determined by fitting the data to the Hill equation using GraphPad Prism 8 software.

**Growth conditions of *Aspergillus niger* strains.** *A. niger* strains used in this study (Table 4) were grown on complete medium (CM) (41) agar (1.5% [wt/vol]) plates at 30°C for 4 days. Spores were harvested with 10 ml of *N*-(2-acetamido)-2-aminoethanesulfonic acid buffer, and 2 $\mu$l of $10^3$ freshly isolated spores was inoculated on MM agar plates. Due to the toxicity of the aromatic compounds, different concentrations were used for the growth profile, i.e., 2 mM for ferulic acid and cinnamic acid and 5 mM for the other compounds. All chemicals were purchased from Sigma-Aldrich.

**Construction of gene deletion cassettes and transformation of *A. niger*.** The gene deletion cassettes were constructed as described previously (46). The flanking regions contained 900 to 1,000 bp upstream and downstream of the gene of interest, including an overlap of the selection marker orotidine 5′-phosphate decarboxylase (*pyrG*) that was amplified from *Aspergillus oryzae* RIB40 (Table 5). These three fragments were combined in a fusion PCR using the GoTaq long PCR master mix (Promega, Madison, WI) as described previously (20). Protoplast-mediated transformation of *A. niger* N593 Δ*kusA* (47) and purification of the different transformants were performed as described before (46). To verify that the phenotypes are not caused by random mutations, three independent deletion mutants were screened for phenotypes (Fig. S5).

**Colorimetric assay for the visualization of phenolic acid degradation in solid media using FeCl₃.** FeCl₃ reacts with many phenolic compounds and is commonly used as a visualization reagent for thin-layer chromatography (48). To visualize if active ShyA was produced by the *shyA* expression strain, LB plates supplemented with 1 mM salicylic acid, 100 $\mu$M IPTG, and 50 $\mu$g/ml of ampicillin were inoculated with 100 $\mu$l of preculture and incubated overnight at 30°C. MM agar plates supplemented with 5 mM salicylic acid, 2,3-dihydroxybenzoic acid, or catechol were inoculated with $10^3$ freshly isolated spores of the Δ*shyA*, Δ*dhbA* or Δ*crcA* mutant and incubated at 30°C for 7 days. After incubation, 5 ml of a 20% FeCl₃ solution was added on the plates for 5 min. Thereafter, the FeCl₃ solution was removed and pictures were taken.

**Phylogenetic analysis.** The amino acid sequence of ShyA was used for BLASTP analysis on selected ascomycete and basidiomycete genomes (Table S3). Mainly industrially relevant species, fungal model species, or fungi that are potentially interesting for new applications were selected. To reduce the

**TABLE 5** Primers used in this study

| Primer | Sequence, 5′[a] | Target |
| --- | --- | --- |
| ShyA-5′F | GGTTCGCTTTGCTTTGCTAGC | 5′ *shyA-pyrG*-flanks |
| ShyA-5′R-pyrG | gcacttaccttcgcattttctggtatattAGGGTTCAATGATGGTTTGAGGT | |
| ShyA-3′F-pyrG | cctgtgttggttctcaggaactgcgaatatGAGTAGATTTCAGGGAGGAGAGC | 3′ *shyA-pyrG*-flanks |
| ShyA-3′R | CTGTTTGTTGCTGAAGCTGTCC | |
| ShyA-Check-F | CCAAGAAAGACTTCCACGTCG | Deletion verification *shyA* |
| ShyA-Check-R | CTTTGCCAGTCGAAAGAATTGG | |
| DbhA-5′F | GCCTTTGGCCGTGATCAG | 5′ *dbhA-pyrG*-flanks |
| DbhA-5′R-pyrG | gcacttaccttcgcattttctggtatattCAGGGATGTGTGAGTAGAGAAGG | |
| DbhA-3′F-pyrG | cctgtgttggttctcaggaactgcgaatatGGCTGACGAGCTAGGATGG | 3′ *dbhA-pyrG*-flanks |
| DbhA-3′R | CAAACAGCCACATGAACAAGCC | |
| DbhA-Check-F | CGAAGAGAAGACGCGCTG | Deletion verification *dhbA* |
| DbhA-Check-R | CTTCTTGCGGTCCTCGAAC | |
| CrcA-5′F | GCAAGGCCACAGCATCAAG | 5′ *crcA-pyrG*-flanks |
| CrcA-5′R-pyrG | gcacttaccttcgcattttctggtatattGTCGAAGCGCGGCATTTTG | |
| CrcA-3′F-pyrG | cctgtgttggttctcaggaactgcgaatatGCGATTGTCTATTGACGTTTGGG | 3′ *crcA-pyrG*-flanks |
| CrcA-3′R | GTCACCGTCAACAACCACC | |
| 4787-Check-F | GCATGGGTCCCAAAACGA | Deletion verification *crcA* |
| 4787-Check-R | CAACTCGAGCAGCTTTCCAG | |
| 43-5′F | CACTACCACAGACCCAGGC | 5′ 43-*pyrG*-flanks |
| 43-5′R-pyrG | gcacttaccttcgcattttctggtatattAGAGAAGTGCTTGCTATGCTGT | |
| 43-3′F-pyrG | cctgtgttggttctcaggaactgcgaatatCATGGTTGTGGGACTGGC | 3′ 43-*pyrG*-flanks |
| 43-3′R | CAAGCGAGCTTCACGTGTC | |
| 43-Check-F | CAACAATCCATCCCCTGCA | Deletion verification 43 |
| 43-Check-R | CTTATTCCATCCCTCGCGGT | |
| 5330-5′F | GCCGTCCATGCCTTTCTCAAG | 5′ 5330-*pyrG*-flanks |
| 5330-5′R-pyrG | gcacttaccttcgcattttctggtatattCCGTTCGATTGTTGCTCAGACAT | |
| 5330-3′F-pyrG | cctgtgttggttctcaggaactgcgaatatCCTCGCAAGACTGAGGATTTGG | 3′ 5330-*pyrG*-flanks |
| 5330-3′R | GCTATCCATCCCGATAAGCATGC | |
| 5330-Check-F | ATCTTGAAGTTGATCCAGGCC | Deletion verification 5330 |
| 5330-Check-R | TAGGAAAGGGCGTCGACG | |
| 2597-5′F | CCAACCAAAACGTGGTCACG | 5′ 2597-*pyrG*-flanks |
| 2597-5′R-pyrG | gcacttaccttcgcattttctggtatattGTACTGAAATGGCCTGACTGGTC | |
| 2597-3′F-pyrG | cctgtgttggttctcaggaactgcgaatatCGTGCTTTTCCAGTTGAGAATGC | 3′ 2597-*pyrG*-flanks |
| 2597-3′R | GTCCAATCCAACCCAGGTGAG | |
| 2597-Check-F | GTCGACGTCCTGATCTGTG | Deletion verification 2597 |
| 2597-Check-R | CCGGATACTGGATTTCTTCCG | |
| pET28-amplification F | CCACTGAGATCCGGCTGCTA | pET28 backbone amplification |
| pET28-amplification R | GCTAGCCATATGGCTGCC | |
| CrcA-amplification F | CTGGTGCCGCGCGGCAGCCATATGGCTAGCCCGCGCTTCGACCCCAAC | *crcA*-6×HIS with pET28 overlap |
| CrcA-amplification R | CGGGCTTTGTTAGCAGCCGGATCTCAGTGGTCAGTTCGCCGGCGCCC | |
| pET28-sequencing primer F | GTGAGCGGATAACAATTCCCCTCTAGAAATA | Confirmation of insert in pET28 vector |
| pET28-sequencing primer R | CCTTTCAGCAAAAAACCCCTCAAGACC | |

[a]In lowercase sequences are regions flanking *pyrG*.

amount of insignificant hits, a cutoff E value of $10^{-40}$ was used. The amino acid sequences of NahG from *P. putida* was included in the phylogenetic analysis as the outgroup (49). The putative salicylate hydroxylase FgShyC and FgNagH from *F. graminearum* were not obtained as homologs through BLASTP and were manually included in the analysis (16, 18). Amino acid sequences were aligned using the MUSCLE algorithm implemented in MEGA7 with the default settings (50). The maximum likelihood, neighbor joining and minimum evolution trees were constructed using MEGA7 with 500 bootstraps.

## SUPPLEMENTAL MATERIAL

Supplemental material is available online only.
**SUPPLEMENTAL FILE 1**, PDF file, 3.6 MB.
**SUPPLEMENTAL FILE 2**, XLSX file, 0.03 MB.

## ACKNOWLEDGMENTS

## REFERENCES

1. Loake G, Grant M. 2007. Salicylic acid in plant defence—the players and protagonists. Curr Opin Plant Biol 10:466–472. https://doi.org/10.1016/j.pbi.2007.08.008.
2. Shah J. 2003. The salicylic acid loop in plant defense. Curr Opin Plant Biol 6:365–371. https://doi.org/10.1016/s1369-5266(03)00058-x.
3. Subba Rao PV, Moore K, Towers GHN. 1967. *o*-Pyrocatechuic acid carboxy-lyase from *Aspergillus niger*. Arch Biochem Biophys 122:466–473. https://doi.org/10.1016/0003-9861(67)90220-2.
4. Milstein O, Vered Y, Shragina L, Gressel J, Flowers HM, Hüttermann A. 1983. Metabolism of lignin related aromatic compounds by *Aspergillus japonicus*. Arch Microbiol 135:147–154. https://doi.org/10.1007/BF00408025.
5. Martins TM, Hartmann DO, Planchon S, Martins I, Renaut J, Silva Pereira C. 2015. The old 3-oxoadipate pathway revisited: new insights in the catabolism of aromatics in the saprophytic fungus *Aspergillus nidulans*. Fungal Genet Biol 74:32–44. https://doi.org/10.1016/j.fgb.2014.11.002.
6. Lubbers RJM, Dilokpimol A, Visser J, Mäkelä MR, Hildén KS, de Vries RP. 2019. A comparison between the homocyclic aromatic metabolic pathways from plant-derived compounds by bacteria and fungi. Biotechnol Adv 37:107396. https://doi.org/10.1016/j.biotechadv.2019.05.002.
7. Santha R, Savithri HS, Rao NA, Vaidyanathan CS. 1995. 2,3-Dihydroxybenzoic acid decarboxylase from *Aspergillus niger*. A novel decarboxylase. Eur J Biochem 230:104–110. https://doi.org/10.1111/j.1432-1033.1995.0104i.x.
8. Wu W, Dutta T, Varman AM, Eudes A, Manalansan B, Loqué D, Singh S. 2017. Lignin valorization: two hybrid biochemical routes for the conversion of polymeric lignin into value-added chemicals. Sci Rep 7:8420. https://doi.org/10.1038/s41598-017-07895-1.
9. Curran KA, Leavitt JM, Karim AS, Alper HS. 2013. Metabolic engineering of muconic acid production in *Saccharomyces cerevisiae*. Metab Eng 15:55–66. https://doi.org/10.1016/j.ymben.2012.10.003.
10. Sun X, Lin Y, Huang Q, Yuan Q, Yan Y. 2013. A novel muconic acid biosynthesis approach by shunting tryptophan biosynthesis via anthranilate. Appl Environ Microbiol 79:4024–4030. https://doi.org/10.1128/AEM.00859-13.
11. Weber C, Brückner C, Weinreb S, Lehr C, Essl C, Boles E. 2012. Biosynthesis of *cis,cis*-muconic acid and its aromatic precursors, catechol and protocatechuic acid, from renewable feedstocks by *Saccharomyces cerevisiae*. Appl Environ Microbiol 78:8421–8430. https://doi.org/10.1128/AEM.01983-12.
12. Barton N, Horbal L, Starck S, Kohlstedt M, Luzhetskyy A, Wittmann C. 2018. Enabling the valorization of guaiacol-based lignin: integrated chemical and biochemical production of *cis,cis*-muconic acid using metabolically engineered *Amycolatopsis* sp ATCC 39116. Metab Eng 45:200–210. https://doi.org/10.1016/j.ymben.2017.12.001.
13. Kohlstedt M, Starck S, Barton N, Stolzenberger J, Selzer M, Mehlmann K, Schneider R, Pleissner D, Rinkel J, Dickschat JS, Venus J, van Duuren BJHJ, Wittmann C. 2018. From lignin to nylon: cascaded chemical and biochemical conversion using metabolically engineered *Pseudomonas putida*. Metab Eng 47:279–293. https://doi.org/10.1016/j.ymben.2018.03.003.
14. Sonoki T, Morooka M, Sakamoto K, Otsuka Y, Nakamura M, Jellison J, Goodell B. 2014. Enhancement of protocatechuate decarboxylase activity for the effective production of muconate from lignin-related aromatic compounds. J Biotechnol 192:71–77. https://doi.org/10.1016/j.jbiotec.2014.10.027.
15. Lin Y, Sun X, Yuan Q, Yan Y. 2014. Extending shikimate pathway for the production of muconic acid and its precursor salicylic acid in *Escherichia coli*. Metab Eng 23:62–69. https://doi.org/10.1016/j.ymben.2014.02.009.
16. Hao G, Naumann TA, Vaughan MM, McCormick S, Usgaard T, Kelly A, Ward TJ. 2019. Characterization of a *Fusarium graminearum* salicylate hydroxylase. Front Microbiol 10:3219. https://doi.org/10.3389/fmicb.2018.03219.
17. Ambrose KV, Tian Z, Wang Y, Smith J, Zylstra G, Huang B, Belanger FC. 2015. Functional characterization of salicylate hydroxylase from the fungal endophyte *Epichloë festucae*. Sci Rep 5:10939. https://doi.org/10.1038/srep10939.
18. Qi PF, Zhang YZ, Liu CH, Chen Q, Guo ZR, Wang Y, Xu BJ, Jiang YF, Zheng T, Gong X, Luo CH, Wu W, Kong L, Deng M, Ma J, Lan XJ, Jiang QT, Wei YM, Wang JR, Zheng YL. 2019. Functional analysis of FgNahG clarifies the contribution of salicylic acid to wheat (*Triticum aestivum*) resistance against fusarium head blight. Toxins (Basel) 11:59. https://doi.org/10.3390/toxins11020059.
19. Semana P, Powlowski J. 2019. Four aromatic intradiol ring cleavage dioxygenases from *Aspergillus niger*. Appl Environ Microbiol 85:e01786-19. https://doi.org/10.1128/AEM.01786-19.
20. Lubbers RJM, Dilokpimol A, Peng M, Visser J, Mäkelä MR, Hildén KS, de Vries RP. 2019. Discovery of novel *p*-hydroxybenzoate-*m*-hydroxylase, protocatechuate 3,4 ring-cleavage dioxygenase and hydroxyquinol 1,2 ring-cleavage dioxygenase from the filamentous fungus *Aspergillus niger*. ACS Sustain Chem Eng 7:19081–19089. https://doi.org/10.1021/acssuschemeng.9b04918.
21. Lubbers RJM, Dilokpimol A, Navarro J, Peng M, Wang M, Lipzen A, Ng V, Grigoriev IV, Visser J, Hildén KS, de Vries RP. 2019. Cinnamic acid and sorbic acid conversion are mediated by the same transcriptional regulator in *Aspergillus niger*. Front Bioeng Biotechnol 7:249. https://doi.org/10.3389/fbioe.2019.00249.
22. White-Stevens RH, Kamin H, Gibson QH. 1972. Studies of a flavoprotein, salicylate hydroxylase. I. Enzyme mechanism. J Biol Chem 247:2371–2381.
23. Balashova NV, Stolz A, Knackmuss HJ, Kosheleva IA, Naumov AV, Boronin AM. 2001. Purification and characterization of a salicylate hydroxylase involved in 1-hydroxy-2-naphthoic acid hydroxylation from the naphthalene and phenanthrene-degrading bacterial strain *Pseudomonas putida* BS202-P1. Biodegradation 12:179–188. https://doi.org/10.1023/a:1013126723719.
24. Rabe F, Ajami-Rashidi Z, Doehlemann G, Kahmann R, Djamei A. 2013. Degradation of the plant defence hormone salicylic acid by the biotrophic fungus *Ustilago maydis*. Mol Microbiol 89:179–188. https://doi.org/10.1111/mmi.12269.
25. Graminha MAS, Rocha EMF, Prade RA, Martinez-Rossi NM. 2004. Terbinafine resistance mediated by salicylate 1-monooxygenase in *Aspergillus nidulans*. Antimicrob Agents Chemother 48:3530–3535. https://doi.org/10.1128/AAC.48.9.3530-3535.2004.
26. Wright JD. 1993. Fungal related degradation compounds of benzoic acid and related compounds. World J Microbiol Biotechnol 9:9–16. https://doi.org/10.1007/BF00656508.
27. Rocheleau H, Al-Harthi R, Ouellet T. 2019. Degradation of salicylic acid by *Fusarium graminearum*. Fungal Biol 123:77–86. https://doi.org/10.1016/j.funbio.2018.11.002.
28. Wang LH, Tu SC. 1984. The kinetic mechanism of salicylate hydroxylase as studied by initial rate measurement, rapid reaction kinetics, and isotope effects. J Biol Chem 259:10682–10688.
29. Qi PF, Johnston A, Balcerzak M, Rocheleau H, Harris LJ, Long XY, Wei YM, Zheng YL, Ouellet T. 2012. Effect of salicylic acid on *Fusarium graminearum*, the major causal agent of fusarium head blight in wheat. Fungal Biol 116:413–426. https://doi.org/10.1016/j.funbio.2012.01.001.
30. Romsdahl J, Wang CCC. 2019. Recent advances in the genome mining of *Aspergillus* secondary metabolites (covering 2012–2018). Medchemcomm 10:840–866. https://doi.org/10.1039/c9md00054b.
31. Rao PV, Moore K, Towers GH. 1967. The conversion of tryptophan to 2,3-dihydroxybenzoic acid and catechol by *Aspergillus niger*. Biochem Biophys Res Commun 28:1008–1012. https://doi.org/10.1016/0006-291X(67)90081-2.
32. Zhang K, Halitschke R, Yin C, Liu CJ, Gan SS. 2013. Salicylic acid 3-hydroxylase regulates *Arabidopsis* leaf longevity by mediating salicylic acid catabolism. Proc Natl Acad Sci U S A 110:14807–14812. https://doi.org/10.1073/pnas.1302702110.
33. Anderson JJ, Dagley S. 1980. Catabolism of aromatic acids in *Trichosporon cutaneum*. J Bacteriol 141:534–543. https://doi.org/10.1128/JB.141.2.534-543.1980.
34. Chou CH, Patrick ZA. 1976. Identification and phytotoxic activity of compounds produced during decomposition of corn and rye residues in soil. J Chem Ecol 2:369–387. https://doi.org/10.1007/BF00988283.
35. Jain R, Singh M, Dezman DJ. 1989. Qualitative and quantitative characterization of phenolic compounds from lantana (*Lantana camara*) leaves. Weed Sci 37:302–307. https://doi.org/10.1017/S0043174500071964.
36. Singh M, Tamma RV, Nigg HN. 1989. HPLC identification of allelopathic compounds from Lantana camara. J Chem Ecol 15:81–89. https://doi.org/10.1007/BF02027775.

37. Siqueira JO, Nair MG, Hammerschmidt R, Safir GR, Putnam AR. 1991. Significance of phenolic compounds in plant-soil-microbial systems. CRC Crit Rev Plant Sci 10:63–121. https://doi.org/10.1080/07352689109382307.

38. Arif T. 2015. Salicylic acid as a peeling agent: a comprehensive review. Clin Cosmet Invest Dermatol 8:455–461. https://doi.org/10.2147/CCID.S84765.

39. Phale PS, Sharma A, Gautam K. 2019. Microbial degradation of xenobiotics like aromatic pollutants from the terrestrial environments, p 259–278. In Prasad MNV, Vithanage M, Kapley A (ed), Pharmaceuticals and personal care products: waste management and treatment technology. Elsevier, Inc, Oxford, United Kingdom.

40. Hadibarata T, Yusoff ARM, Aris A, Kristanti RA. 2012. Identification of naphthalene metabolism by white rot fungus Armillaria sp. F022. J Environ Sci 24:728–732. https://doi.org/10.1016/S1001-0742(11)60843-7.

41. de Vries RP, Visser J. 1999. Regulation of the feruloyl esterase (faeA) gene from Aspergillus niger. Appl Environ Microbiol 65:5500–5503. https://doi.org/10.1128/AEM.65.12.5500-5503.1999.

42. Jacobus AP, Gross J. 2015. Optimal cloning of PCR fragments by homologous recombination in Escherichia coli. PLoS One 10:e0119221. https://doi.org/10.1371/journal.pone.0119221.

43. Schneider CA, Rasband WS, Eliceiri KW. 2012. NIH Image to ImageJ: 25 years of image analysis. Nat Methods 9:671–675. https://doi.org/10.1038/nmeth.2089.

44. Dilokpimol A, Mäkelä MR, Mansouri S, Belova O, Waterstraat M, Bunzel M, de Vries RP, Hildén KS. 2017. Expanding the feruloyl esterase gene family of Aspergillus niger by characterization of a feruloyl esterase, FaeC. N Biotechnol 37:200–209. https://doi.org/10.1016/j.nbt.2017.02.007.

45. McIlvaine TC. 1921. A buffer solution for colorimetric comparison. J Biol Chem 49:183–186.

46. Kowalczyk JE, Lubbers RJM, Peng M, Battaglia E, Visser J, De Vries RP. 2017. Combinatorial control of gene expression in Aspergillus niger grown on sugar beet pectin. Sci Rep 7:12356. https://doi.org/10.1038/s41598-017-12362-y.

47. Meyer V, Arentshorst M, El-Ghezal A, Drews AC, Kooistra R, van den Hondel C, Ram AFJ. 2007. Highly efficient gene targeting in the Aspergillus niger kusA mutant. J Biotechnol 128:770–775. https://doi.org/10.1016/j.jbiotec.2006.12.021.

48. Waldi D. 1965. Spray reagents for thin-layer chromatography, p 483–502. In Stahl E (ed), Thin-layer chromatography. Springer, Berlin, Germany.

49. You IS, Murray RI, Jollie D, Gunsalus IC. 1990. Purification and characterization of salicylate hydroxylase from Pseudomonas putida PpG7. Biochem Biophys Res Commun 169:1049–1054. https://doi.org/10.1016/0006-291x(90)92000-p.

50. Kumar S, Stecher G, Tamura K. 2016. MEGA7: Molecular Evolutionary Genetics Analysis version 7.0 for bigger datasets. Mol Biol Evol 33:1870–1874. https://doi.org/10.1093/molbev/msw054.

51. Love MI, Huber W, Anders S. 2014. Moderated estimation of fold change and dispersion for RNA-seq data with DESeq2. Genome Biol 15:550. https://doi.org/10.1186/s13059-014-0550-8.